

A discrete contact model for crowd motion

Bertrand Maury
Université de Paris-Sud
UMR du CNRS 8628
F-91405 Orsay Cedex
bertrand.maury@math.u-psud.fr

Juliette Venel
Université de Paris-Sud
UMR du CNRS 8628
F-91405 Orsay Cedex
juliette.venel@math.u-psud.fr

Abstract

The aim of this paper is to develop a crowd motion model designed to handle highly packed situations. The model we propose rests on two principles: We first define a spontaneous velocity which corresponds to the velocity each individual would like to have in the absence of other people; The actual velocity is then computed as the projection of the spontaneous velocity onto the set of admissible velocities (i.e. velocities which do not violate the non-overlapping constraint). We describe here the underlying mathematical framework, and we explain how recent results by J.F. Edmond and L. Thibault on the sweeping process by uniformly prox-regular sets can be adapted to handle this situation in terms of well-posedness. We propose a numerical scheme for this contact dynamics model, based on a prediction-correction algorithm. Numerical illustrations are finally presented and discussed.

Résumé

Nous proposons un modèle de mouvements de foule orienté vers la gestion de configurations très denses. Ce modèle repose sur deux principes: tout d'abord nous définissons une vitesse souhaitée correspondant à la vitesse que les individus aimeraient avoir en l'absence des autres; la vitesse réelle est alors obtenue comme projection de la vitesse souhaitée sur un ensemble de vitesses admissibles (i.e. qui respectent la contrainte de non-chevauchement). Nous décrivons le cadre mathématique sous-jacent et nous expliquons comment certains résultats de J.F. Edmond et L. Thibault sur les processus de rafle par des ensembles uniformément prox-réguliers peuvent être utilisés pour prouver le caractère bien posé de notre modèle. Nous proposons un schéma numérique pour ce modèle de dynamique des contacts basé sur un algorithme de type prédiction-correction. Enfin des résultats numériques sont présentés et commentés.

Introduction

Walking behaviour of pedestrians has given rise to a large amount of empirical studies over the last decades. Qualitative data (preferences, walk tendencies) have been collected by Fruin [15], Navin, Wheeler [37], Henderson [20] and, more recently, by Weidmann [43]. From these observations, several strategies for crowd motion modelling have been proposed, and can be classified with respect to the way they handle people density (Lagrangian description of individuals or macroscopic approach), and to the nature of motion phenomena (deterministic or stochastic). Among discrete and stochastic models, let us mention Cellular Automata [2, 7, 36, 38], models based on networks [16] as route choice models [3, 4] and queuing models [31, 44]. In these models, each cell or node is either empty or occupied by a single person and people's motion always satisfies this rule. In cellular automata models, there are two manners of moving people during a time step. With the first one, positions are updated one by one with a random order (*Random Sequential Update*). The second method consists of updating simultaneously all positions (*Parallel Update*). If several people want to reach the same cell, only one of them (randomly chosen) is allowed to move. In route choice models, people move on a network. Each model is based on a route choice set. Most choice set generation procedures are based on shortest route search and use shortest paths algorithms. Queuing models use Markov-chain models to describe how pedestrians move from one node of the network to another.

In [19], a microscopic model called social force model is presented. It describes crowd motion with a system of differential equations. The acceleration of an individual is obtained according to Newton's law. Several forces

are introduced as for example a term describing the acceleration towards the desired velocity or a repulsion force reflecting that a pedestrian tends to keep a certain distance from other people and obstacles. Moreover macroscopic models have been proposed. In [20], pedestrian traffic dynamics is firstly compared with fluid dynamics. Some models [17, 20, 22] are based on gas-kinetic theory. Other models [23, 24, 25, 26] rest on a set of partial differential equations describing the conservation of flow equation.

Several softwares have been developed: PedGo [21], SimPed [11], Legion [40], Mipsim [22] or Exodus [16]. Some commonly observed collective patterns are now considered as standard benchmarks for those numerical simulations. Among these phenomena of self-organization, there is the formation of lanes formed naturally by people moving in opposite directions. In this way, strong interactions with oncoming pedestrians are reduced, and a higher walking speed is possible. Another phenomena is the formation of arches upstream the exit during the evacuation of a room. These patterns are recovered by CA-models [28, 39] and by the social force model [19, 18].

The case of evacuation in emergency situations is of particular importance in terms of applications (observance of security rules, computer-assisted design of public buildings, appropriate positioning of exit signs). Numerical simulations may allow to estimate evacuation time (to be compared for example with the duration of fire propagation) and also to predict areas where high density will appear. As pointed out by Helbing [18], emergency situations do not fit into the standard framework of pedestrian traffic flow. When people stroll around without hurry, they tend to keep a certain distance from each other and from obstacles. In an emergency situation, the motion of individuals is governed by different rules. In particular, the contact with walls or other people is no longer avoided. Some strategies have been proposed to adapt social walk models to highly congested situation (see again [18]). We propose here an approach which relies on the very consideration that actual motion in emergency situations is governed by the opposition between achievement of individual satisfaction (people struggle to escape as quickly as possible, regardless of the global efficiency) and congestion. In particular, we aim at integrating the direct conflict between people in the model, in order to estimate in some way interaction forces between them, and therefore provide a way to estimate the local risk of casualties.

The microscopic model we propose rests on two principles. On the one hand, each individual has a spontaneous velocity that he would like to have in the absence of other people. On the other hand, the actual velocity must take into account congestion. Those two principles lead us to define the actual velocity field as the projection of the spontaneous velocity onto the set of admissible velocities (regarding the non-overlapping constraints). The flexibility of this model lies in its first point: every choice of spontaneous velocity can be made and so every existing model for predicting crowd motion can be integrated here. The key feature of the model is the second point which concerns handling of contacts.

By specifying the link between these two velocities, the evolution problem takes the form of a first order differential inclusion. This type of evolution problem has been extensively studied in the 1970's, with the theory of maximal monotone operators (see e.g. [6]). A few years later, J.J. Moreau considered similar problems with time-dependent multivalued operator, namely sweeping processes by convex sets (see [35]). Since then, important improvements have been developed by weakening the convexity assumption with the concept of prox-regularity. The well-posedness of our evolution problem can be established by means of recent results of J.F. Edmond and L. Thibault [13] concerning sweeping processes by uniformly prox-regular sets.

The paper is structured as follows: In Section 2, we present the model and establish its well-posedness; In Section 3, we propose a numerical scheme, and detail the overall solution method. Section 4 is devoted to some illustrations of the numerical algorithm.

1 Modelling

We consider N persons identified to rigid disks. For convenience, the disks are supposed here to have the same radius r . The centre of the i -th disk is denoted by \mathbf{q}_i (see Fig. 1). Since overlapping is forbidden, the vector of positions $\mathbf{q} = (\mathbf{q}_1, \dots, \mathbf{q}_N) \in \mathbb{R}^{2N}$ (equipped with the euclidean norm) is required to belong to the following set:

Definition 1.1 (Set of feasible configurations)

$$Q = \{ \mathbf{q} \in \mathbb{R}^{2N}, D_{ij}(\mathbf{q}) \geq 0 \quad \forall i < j \},$$

where $D_{ij}(\mathbf{q}) = |\mathbf{q}_i - \mathbf{q}_j| - 2r$ is the signed distance between disks i and j .

We consider as given the vector of spontaneous velocities denoted by

$$\mathbf{U}(\mathbf{q}) = (\mathbf{U}_1(\mathbf{q}), \dots, \mathbf{U}_N(\mathbf{q})) \in \mathbb{R}^{2N}.$$

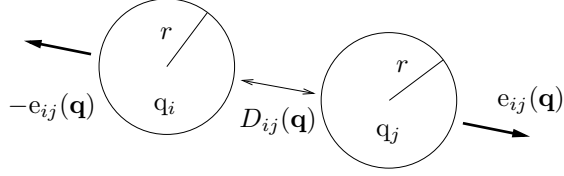


Figure 1: Notations.

\mathbf{U}_i is the spontaneous velocity of individual i , which may depend on its own position ($\mathbf{U}_i = \mathbf{U}_i(\mathbf{q}_i)$, see Section 4 for examples of such a situation), but also on other people's positions, that is why we keep here $\mathbf{U}_i = \mathbf{U}_i(\mathbf{q})$. To define the actual velocity, we introduce the following set:

Definition 1.2 (*Set of feasible velocities*)

$$\mathcal{C}_{\mathbf{q}} = \{ \mathbf{v} \in \mathbb{R}^{2N}, \forall i < j \quad D_{ij}(\mathbf{q}) = 0 \Rightarrow \mathbf{G}_{ij}(\mathbf{q}) \cdot \mathbf{v} \geq 0 \},$$

with

$$\mathbf{G}_{ij}(\mathbf{q}) = \nabla D_{ij}(\mathbf{q}) = (0, \dots, 0, -\mathbf{e}_{ij}(\mathbf{q}), 0, \dots, 0, \mathbf{e}_{ij}(\mathbf{q}), 0, \dots, 0) \in \mathbb{R}^{2N} \text{ and } \mathbf{e}_{ij}(\mathbf{q}) = \frac{\mathbf{q}_j - \mathbf{q}_i}{|\mathbf{q}_j - \mathbf{q}_i|}.$$

The actual velocity field is defined as the feasible field which is the closest to \mathbf{U} in the least square sense, which writes

$$\begin{cases} \frac{d\mathbf{q}}{dt} = P_{\mathcal{C}_{\mathbf{q}}} \mathbf{U}(\mathbf{q}), \\ \mathbf{q}(0) = \mathbf{q}_0 \in Q, \end{cases} \quad (1)$$

where $P_{\mathcal{C}_{\mathbf{q}}}$ denotes the euclidean projection onto the closed convex cone $\mathcal{C}_{\mathbf{q}}$.

Remark 1.3 *Despite its formal simplicity, this model does not fit directly into a standard framework. Indeed the set $\mathcal{C}_{\mathbf{q}}$ does not continuously depend on \mathbf{q} . If no contact holds, the velocity is not constrained and $\mathcal{C}_{\mathbf{q}} = \mathbb{R}^{2N}$. With a single contact, the set $\mathcal{C}_{\mathbf{q}}$ becomes a half-space.*

2 Mathematical framework

2.1 Reformulation

Let us reformulate the problem by introducing $\mathcal{N}_{\mathbf{q}}$, the outward normal cone to the set of feasible configurations Q , which is defined as the polar cone of $\mathcal{C}_{\mathbf{q}}$.

Definition 2.1 (*Outward normal cone*)

$$\mathcal{N}_{\mathbf{q}} = \mathcal{C}_{\mathbf{q}}^{\circ} = \{ \mathbf{w} \in \mathbb{R}^{2N}, \mathbf{w} \cdot \mathbf{v} \leq 0 \quad \forall \mathbf{v} \in \mathcal{C}_{\mathbf{q}} \}.$$

Remark 2.2 *In Figure 2, we represent the set $Q \subset \mathbb{R}^{2N}$ which is defined as an intersection of convex sets' complements. In the case of a single contact (configuration \mathbf{q}_1), we remark that the cone $\mathcal{N}_{\mathbf{q}_1}$ is generated by the vector $-\mathbf{G}_{34}(\mathbf{q}_1)$ that is up to a constant, the outward normal vector to the domain $D_{34} \geq 0$. In the case of two or more contacts, the configuration \mathbf{q}_2 does not belong to a smooth surface and the cone $\mathcal{N}_{\mathbf{q}_2}$ (generated by $-\mathbf{G}_{12}(\mathbf{q}_2)$ and $-\mathbf{G}_{13}(\mathbf{q}_2)$) generalizes somehow the notion of the outward normal direction.*

Thanks to Farkas' Lemma (see [8]), the outward normal cone can be expressed

$$\mathcal{N}_{\mathbf{q}} = \left\{ -\sum \lambda_{ij} \mathbf{G}_{ij}(\mathbf{q}), \lambda_{ij} \geq 0, D_{ij}(\mathbf{q}) > 0 \implies \lambda_{ij} = 0 \right\}. \quad (2)$$

Let us recall the classical orthogonal decomposition of a Hilbert space as the sum of mutually polar cone (see [34]) :

$$P_{\mathcal{C}_{\mathbf{q}}} + P_{\mathcal{N}_{\mathbf{q}}} = Id. \quad (3)$$

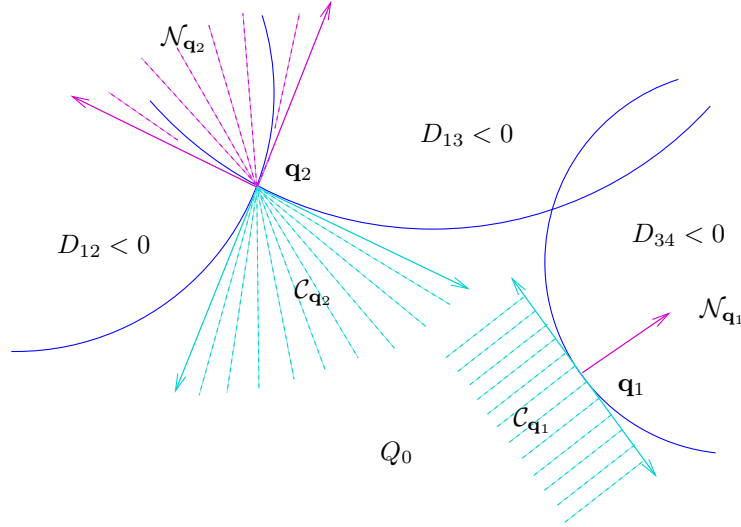


Figure 2: Cones $\mathcal{C}_{\mathbf{q}}$ and $\mathcal{N}_{\mathbf{q}}$.

Using this property, we get:

$$\frac{d\mathbf{q}}{dt} = P_{\mathcal{C}_{\mathbf{q}}} \mathbf{U}(\mathbf{q}) = \mathbf{U}(\mathbf{q}) - P_{\mathcal{N}_{\mathbf{q}}} \mathbf{U}(\mathbf{q}). \quad (4)$$

Since $P_{\mathcal{N}_{\mathbf{q}}} \mathbf{U}(\mathbf{q}) \in \mathcal{N}_{\mathbf{q}}$, we obtain a new formulation for (1)

$$\begin{cases} \frac{d\mathbf{q}}{dt} + \mathcal{N}_{\mathbf{q}} \ni \mathbf{U}(\mathbf{q}), \\ \mathbf{q}(0) = \mathbf{q}_0. \end{cases} \quad (5)$$

The problem reads as a first order differential inclusion involving the multivalued operator \mathcal{N} .

Remark 2.3 *In the absence of contacts in the configuration \mathbf{q} , the set of feasible velocities $\mathcal{C}_{\mathbf{q}}$ is equal to the whole space \mathbb{R}^{2N} , and consequently the outward normal cone $\mathcal{N}_{\mathbf{q}}$ is reduced to $\{0\}$. In that case, the first relation of (5) states that the actual velocity equals to the spontaneous velocity:*

$$\frac{d\mathbf{q}}{dt} = \mathbf{U}(\mathbf{q}).$$

If any contact exists, the differential inclusion means that the configuration \mathbf{q} , submitted to $\mathbf{U}(\mathbf{q})$, has to evolve while remaining in Q .

Let us first study a special situation where standard theory can be applied. Consider N individuals in a corridor. In that case, as people cannot leap across each other, it is natural to restrict the set of feasible configurations to one of its connected components:

$$Q = \{\mathbf{q} = (q_1, \dots, q_N) \in \mathbb{R}^N, q_{i+1} - q_i \geq 2r\}.$$

In this very situation, as Q is closed and convex, the multivalued operator $\mathbf{q} \mapsto \mathcal{N}_{\mathbf{q}}$ identifies to the subdifferential of the indicatrix function of Q :

$$\partial I_Q(\mathbf{q}) = \{\mathbf{v}, I_Q(\mathbf{q}) + (\mathbf{v}, \mathbf{h}) \leq I_Q(\mathbf{q} + \mathbf{h}) \quad \forall \mathbf{h}\}, \quad I_Q(\mathbf{q}) = \begin{cases} 0 & \text{if } \mathbf{q} \in Q \\ +\infty & \text{if } \mathbf{q} \notin Q \end{cases}$$

therefore $\mathbf{q} \mapsto \mathcal{N}_{\mathbf{q}}$ is maximal monotone. In that case, as soon as the spontaneous velocity is regular (say Lipschitz), standard theory (see e.g. Brezis [6]) ensures well-posedness. Yet, as illustrated in Figure 3, Q is not convex in general and the operator $\mathbf{q} \mapsto \mathcal{N}_{\mathbf{q}}$ is not monotone. So we cannot apply the same arguments as in the case of a straight motion. By lack of convexity, the projection onto Q is not everywhere well-defined. However the set Q satisfies a weaker property in the sense that the projection onto Q is still well-defined in its neighbourhood. Indeed, Q is uniformly prox-regular, which is the suitable property to ensure well-posedness. Let us give some definitions to specify the general mathematical framework.

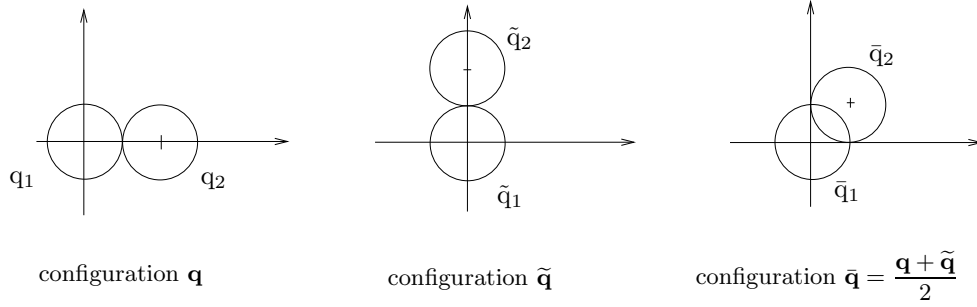


Figure 3: Lack of convexity.

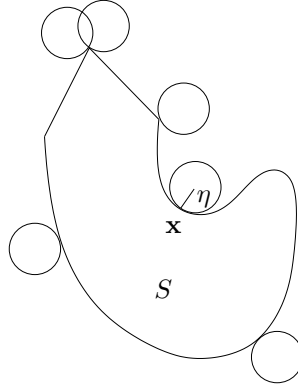


Figure 4: η -prox-regular set.

Definition 2.4 Let S be a closed subset of a Hilbert space H . We define the proximal normal cone to S at \mathbf{x} by:

$$N(S, \mathbf{x}) = \{ \mathbf{v} \in H, \exists \alpha > 0, \mathbf{x} \in P_S(\mathbf{x} + \alpha \mathbf{v}) \},$$

where

$$P_S(\mathbf{y}) = \{ \mathbf{z} \in S, d_S(\mathbf{y}) = |\mathbf{y} - \mathbf{z}| \}, \text{ with } d_S(\mathbf{y}) = \min_{\mathbf{z} \in S} |\mathbf{y} - \mathbf{z}|.$$

Following [10], we define the concept of uniform prox-regularity as follows:

Definition 2.5 Let S be a closed subset of a Hilbert space H . S is said η -prox-regular if for all $\mathbf{x} \in \partial S$ and $\mathbf{v} \in N(S, \mathbf{x})$, $|\mathbf{v}| = 1$ we have:

$$B(\mathbf{x} + \eta \mathbf{v}, \eta) \cap S = \emptyset.$$

In an euclidean space, S is η -prox-regular if an external tangent ball with radius smaller than η can be rolled around it (see Fig 4). Moreover, this definition ensures that the projection onto such a set is well-defined in its neighbourhood. The following remark will be useful later.

Remark 2.6 If there exists $\alpha > 0$ satisfying $\mathbf{x} \in P_S(\mathbf{x} + \alpha \mathbf{v})$ then

$$\forall \beta \geq 0, \beta \leq \alpha, \mathbf{x} \in P_S(\mathbf{x} + \beta \mathbf{v}).$$

Definition 2.7 The proximal subdifferential of function d_S at \mathbf{x} is the set

$$\partial^P d_S(\mathbf{x}) = \left\{ \mathbf{v} \in H, \exists M, \alpha > 0, d_S(\mathbf{y}) - d_S(\mathbf{x}) + M|\mathbf{y} - \mathbf{x}|^2 \geq \langle \mathbf{v}, \mathbf{y} - \mathbf{x} \rangle, \forall \mathbf{y} \in B(\mathbf{x}, \alpha) \right\}.$$

Let us specify the useful link between the previous subdifferential and the proximal normal cone, which is proved in [5, 9].

Proposition 2.8 *The following relation holds true:*

$$\partial^P d_S(\mathbf{x}) = N^P(S, \mathbf{x}) \cap \overline{B(0, 1)}.$$

Remark 2.9 *A set $C \subset H$ is convex if and only if it is ∞ -prox-regular. In this case $N(C, \mathbf{x}) = \partial I_C(\mathbf{x})$ for all $\mathbf{x} \in C$.*

We now come to the main result of this section.

Theorem 2.10 *Assume that \mathbf{U} is Lipschitz and bounded. Then, for all $T > 0$ and all $\mathbf{q}_0 \in Q$, the following problem*

$$\begin{cases} \frac{d\mathbf{q}}{dt} + \mathcal{N}_{\mathbf{q}} \ni \mathbf{U}(\mathbf{q}) \\ \mathbf{q}(0) = \mathbf{q}_0, \end{cases}$$

has one and only one absolutely continuous solution $\mathbf{q}(\cdot)$ over $[0, T]$.

This well-posedness can be obtained by using results in [13, 14] as soon as we prove that Q is uniformly prox-regular and that the set $\mathcal{N}_{\mathbf{q}}$ identifies to the proximal normal cone to Q at \mathbf{q} . This is the core of next subsection.

Remark 2.11 *It can be shown that the solution given by Theorem 2.10 satisfies the initial differential equation (4) (see [1]).*

2.2 Prox-regularity of Q

Let us consider the set

$$Q_{ij} = \{\mathbf{q} \in \mathbb{R}^{2N}, D_{ij}(\mathbf{q}) \geq 0\}.$$

Proposition 2.12 *Let S be a closed subset of \mathbb{R}^n whose boundary ∂S is an oriented C^2 hypersurface. For each $\mathbf{x} \in \partial S$, we denote by $\nu(\mathbf{x})$ the outward normal to S at \mathbf{x} . Then, for each $\mathbf{x} \in \partial S$, the proximal normal cone to S at \mathbf{x} is generated by $\nu(\mathbf{x})$, i.e.*

$$N(S, \mathbf{x}) = \mathbb{R}^+ \nu(\mathbf{x}).$$

Proof: The proof is a straightforward computation (see [41]). □

We can also deduce the expression of the proximal normal cone to Q_{ij} .

Corollary 2.13 *For all $\mathbf{q} \in Q_{ij}$,*

$$N(Q_{ij}, \mathbf{q}) = -\mathbb{R}^+ \mathbf{G}_{ij}(\mathbf{q}).$$

By Definition 2.5, the constant of prox-regularity equals to the largest radius of a “rolling external ball”. In order to estimate its radius, tools of differential geometry can be used. More precisely, to show that the set Q_{ij} is uniformly prox-regular, we can apply the following theorem, that is proved in [12].

Theorem 2.14 *Let C be a closed convex subset of \mathbb{R}^n such that ∂C is an oriented C^2 hypersurface of \mathbb{R}^n . We denote by $\nu_C(\mathbf{x})$ the outward normal to C at \mathbf{x} and by $\rho_1(\mathbf{x}), \dots, \rho_{n-1}(\mathbf{x}) \geq 0$ the principal curvatures of C at \mathbf{x} . We suppose that*

$$\rho = \sup_{\mathbf{x} \in \partial C} \sup_{1 \leq i \leq n-1} \rho_i(\mathbf{x}) < \infty.$$

Then $S = \mathbb{R}^n \setminus \text{int}(C)$ is a η -prox-regular set with $\eta = \frac{1}{\rho}$.

Proposition 2.15 *Q_{ij} is η_0 -prox-regular with $\eta_0 = r\sqrt{2}$.*

Proof: The set $\text{int}(Q_{ij})$ is obviously the complement of a convex set C which satisfies the assumptions of Theorem 2.14. The constant of prox-regularity of Q_{ij} can be obtained by calculating its principal curvatures, which are the eigenvalues of Weingarten endomorphism. Let $\mathbf{q} \in \partial Q_{ij}$, the outward normal to C at \mathbf{q} is equal to $-\nu(\mathbf{q})$, where

$$\nu(\mathbf{q}) = -\frac{\mathbf{G}_{ij}(\mathbf{q})}{\sqrt{2}} = \frac{(0, \dots, 0, e_{ij}(\mathbf{q}), 0, \dots, 0, -e_{ij}(\mathbf{q}), 0, \dots, 0)}{\sqrt{2}}.$$

Weingarten endomorphism is written as follows, for all tangent vectors $\mathbf{h} \in T_{\mathbf{q}}(\partial Q_{ij})$,

$$\mathbf{W}_{\mathbf{q}}(\mathbf{h}) := -D\nu(\mathbf{q})[\mathbf{h}] = \frac{1}{\sqrt{2}|\mathbf{q}_j - \mathbf{q}_i|} \left(0, \dots, 0, -P_{e_{ij}^\perp}(\mathbf{h}_j - \mathbf{h}_i), 0, \dots, 0, P_{e_{ij}^\perp}(\mathbf{h}_j - \mathbf{h}_i), 0, \dots, 0 \right),$$

with

$$P_{e_{ij}^\perp}(\mathbf{h}_j - \mathbf{h}_i) = (\mathbf{h}_j - \mathbf{h}_i) - [(\mathbf{h}_j - \mathbf{h}_i) \cdot e_{ij}]e_{ij}.$$

After some computations, we deduce that the endomorphism $\mathbf{W}_{\mathbf{q}}$ has two eigenvalues, 0 and $\sqrt{2}/|\mathbf{q}_j - \mathbf{q}_i|$, and the latter is equal to $1/(r\sqrt{2})$, which ends the proof. \square

Now let us study the set of feasible configurations Q , that is the intersection of all sets Q_{ij} . We begin to determine its proximal normal cone.

Proposition 2.16 For all $\mathbf{q} \in Q$, $N(Q, \mathbf{q}) = \sum N(Q_{ij}, \mathbf{q}) = \mathcal{N}_{\mathbf{q}}$.

Proof: The second equality follows from (2) and Proposition 2.15. Let us prove the first one. If $\mathbf{q} \in \text{int}(Q)$, then for each couple (i, j) , $\mathbf{q} \in \text{int}(Q_{ij})$, which implies

$$N(Q, \mathbf{q}) = \{0\} = \sum N(Q_{ij}, \mathbf{q}).$$

We now consider $\mathbf{q} \in \partial Q$ and introduce the following set:

$$I_{\text{contact}} = \{(i, j), i < j, D_{ij}(\mathbf{q}) = 0\} = \{(i, j), i < j, \mathbf{q} \in \partial Q_{ij}\}. \quad (6)$$

First, we check that $N(Q_{ij}, \mathbf{q}) \subset N(Q, \mathbf{q})$. Let (i, j) belong to I_{contact} (otherwise the previous inclusion is obvious), we consider $\mathbf{w} \in N(Q_{ij}, \mathbf{q}) \setminus \{0\}$ and we set $\mathbf{v} = \mathbf{w}/|\mathbf{w}|$. By Proposition 2.8, $\mathbf{v} \in \partial^P d_{Q_{ij}}(\mathbf{q})$ and thus

$$\exists M, \alpha > 0, d_{Q_{ij}}(\tilde{\mathbf{q}}) - d_{Q_{ij}}(\mathbf{q}) + M|\tilde{\mathbf{q}} - \mathbf{q}|^2 \geq \mathbf{v} \cdot (\tilde{\mathbf{q}} - \mathbf{q}), \forall \tilde{\mathbf{q}} \in B(\mathbf{q}, \alpha).$$

Since $d_{Q_{ij}}(\mathbf{q}) = 0 = d_Q(\mathbf{q})$ and $d_{Q_{ij}}(\tilde{\mathbf{q}}) \leq d_Q(\tilde{\mathbf{q}})$, it follows that

$$\exists M, \alpha > 0, d_Q(\tilde{\mathbf{q}}) - d_Q(\mathbf{q}) + M|\tilde{\mathbf{q}} - \mathbf{q}|^2 \geq \mathbf{v} \cdot (\tilde{\mathbf{q}} - \mathbf{q}), \forall \tilde{\mathbf{q}} \in B(\mathbf{q}, \alpha).$$

Therefore $\mathbf{v} \in \partial^P d_Q(\mathbf{q})$ and $\mathbf{w} \in N(Q, \mathbf{q})$. Consequently, for each couple $(i, j) \in I_{\text{contact}}$, we obtain $N(Q_{ij}, \mathbf{q}) \subset N(Q, \mathbf{q})$ as required. We now want to prove

$$\sum N(Q_{ij}, \mathbf{q}) \subset N(Q, \mathbf{q}).$$

It suffices to show that

$$\forall \mathbf{w}_1, \mathbf{w}_2 \in N(Q, \mathbf{q}) \setminus \{0\}, \mathbf{w} = \mathbf{w}_1 + \mathbf{w}_2 \in N(Q, \mathbf{q}).$$

Let \mathbf{w}_1 and \mathbf{w}_2 belong to $N(Q, \mathbf{q}) \setminus \{0\}$, we set $\mathbf{w} = \mathbf{w}_1 + \mathbf{w}_2$, $\mathbf{v}_1 = \mathbf{w}_1/|\mathbf{w}_1|$ and $\mathbf{v}_2 = \mathbf{w}_2/|\mathbf{w}_2|$. By Proposition 2.8, there exists $M_1, M_2 \geq 0, \alpha_1, \alpha_2 > 0$ such that

$$d_Q(\tilde{\mathbf{q}}) - d_Q(\mathbf{q}) + M_1|\tilde{\mathbf{q}} - \mathbf{q}|^2 \geq \langle \mathbf{v}_1, \tilde{\mathbf{q}} - \mathbf{q} \rangle, \forall \tilde{\mathbf{q}} \in B(\mathbf{q}, \alpha_1),$$

$$d_Q(\tilde{\mathbf{q}}) - d_Q(\mathbf{q}) + M_2|\tilde{\mathbf{q}} - \mathbf{q}|^2 \geq \langle \mathbf{v}_2, \tilde{\mathbf{q}} - \mathbf{q} \rangle, \forall \tilde{\mathbf{q}} \in B(\mathbf{q}, \alpha_2).$$

So $\mathbf{w} = |\mathbf{w}_1|\mathbf{v}_1 + |\mathbf{w}_2|\mathbf{v}_2$ and the vector $\mathbf{v} = \mathbf{w}/|\mathbf{w}| + |\mathbf{w}_2|$ satisfies $|\mathbf{v}| \leq 1$. Furthermore $\mathbf{v} = t\mathbf{v}_1 + (1-t)\mathbf{v}_2$, where

$$t = \frac{|\mathbf{w}_1|}{(|\mathbf{w}_1| + |\mathbf{w}_2|)}.$$

For $\alpha = \min(\alpha_1, \alpha_2)$ and $M = tM_1 + (1-t)M_2$, the following relation holds

$$d_Q(\tilde{\mathbf{q}}) - d_Q(\mathbf{q}) + M|\tilde{\mathbf{q}} - \mathbf{q}|^2 \geq \mathbf{v} \cdot (\tilde{\mathbf{q}} - \mathbf{q}), \forall \tilde{\mathbf{q}} \in B(\mathbf{q}, \alpha).$$

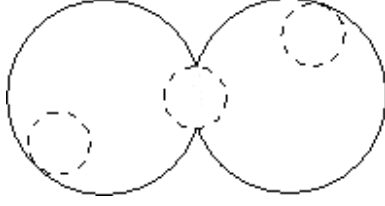


Figure 5: Vanishing of the constant of prox-regularity.

Hence $\mathbf{v} \in \partial^P d_Q(\mathbf{q})$ and $\mathbf{w} \in N(Q, \mathbf{q})$. To conclude, it remains to check that

$$N(Q, \mathbf{q}) \subset \sum N(Q_{ij}, \mathbf{q}).$$

By (3), any $\mathbf{w} \in N(Q, \mathbf{q})$ can be written $\mathbf{w} = \mathbf{v} + \mathbf{z} = P_{\mathcal{N}_q} \mathbf{w} + P_{\mathcal{C}_q} \mathbf{w}$, with $\mathbf{v} \perp \mathbf{z}$. Suppose $\mathbf{z} \neq 0$. Since $\mathbf{w} \in N(Q, \mathbf{q})$, there exists $t > 0$ such that $\mathbf{q} \in P_Q(\mathbf{q} + t\mathbf{w})$. Let

$$s = \min(t, \epsilon) \text{ with } \epsilon = \min_{(i,j) \notin I_{\text{contact}}} \frac{D_{ij}(\mathbf{q})}{\sqrt{2}|\mathbf{z}|},$$

by Remark 2.6, we know that $\mathbf{q} \in P_Q(\mathbf{q} + s\mathbf{w})$. Now set

$$\tilde{\mathbf{q}} = \mathbf{q} + s\mathbf{w} - s\mathbf{v} = \mathbf{q} + s\mathbf{z}$$

and show that $\tilde{\mathbf{q}} \in Q$. By convexity of D_{ij} , we have

$$D_{ij}(\tilde{\mathbf{q}}) \geq D_{ij}(\mathbf{q}) + s \mathbf{G}_{ij}(\mathbf{q}) \cdot \mathbf{z}, \quad \forall (i, j).$$

In addition, for $(i, j) \in I_{\text{contact}}$, it yields $\mathbf{G}_{ij}(\mathbf{q}) \cdot \mathbf{z} \geq 0$, because $\mathbf{z} \in \mathcal{C}_q$. Consequently,

$$\forall (i, j) \in I_{\text{contact}}, D_{ij}(\tilde{\mathbf{q}}) \geq D_{ij}(\mathbf{q}) + s \mathbf{G}_{ij}(\mathbf{q}) \cdot \mathbf{z} = s \mathbf{G}_{ij}(\mathbf{q}) \cdot \mathbf{z} \geq 0.$$

Furthermore, if $(i, j) \notin I_{\text{contact}}$, then $s \leq \frac{D_{ij}(\mathbf{q})}{\sqrt{2}|\mathbf{z}|}$. Hence

$$D_{ij}(\tilde{\mathbf{q}}) \geq D_{ij}(\mathbf{q}) + s \mathbf{G}_{ij}(\mathbf{q}) \cdot \mathbf{z} \geq D_{ij}(\mathbf{q}) - s\sqrt{2}|\mathbf{z}| \geq 0.$$

That is why $\tilde{\mathbf{q}} \in Q$ and $d_Q(\mathbf{q} + s\mathbf{w}) \leq |\mathbf{q} + s\mathbf{w} - \tilde{\mathbf{q}}| = s|\mathbf{v}|$. Yet $|\mathbf{q} + s\mathbf{w} - \mathbf{q}| = s|\mathbf{w}| > s|\mathbf{v}|$ because $|\mathbf{w}|^2 = |\mathbf{v}|^2 + |\mathbf{z}|^2$. Thus $\mathbf{q} \notin P_Q(\mathbf{q} + s\mathbf{w})$, which leads to a contradiction. In conclusion, $\mathbf{z} = 0$ and $\mathbf{w} = \mathbf{v} \in \mathcal{N}_q = \sum N(Q_{ij}, \mathbf{q})$, which completes the proof of the proposition. \square

Now we want to show the uniform prox-regularity of Q . Since Q does not satisfy the same smoothness properties as Q_{ij} , the results of differential geometry cannot be applied. By Theorem 2.14, if a set is the complement of a smooth convex set, then it is uniformly prox-regular. A natural question arises : Is the intersection of such sets (which is the case for Q) uniformly prox-regular with a constant depending only on the constants of prox-regularity of the smooth sets. From a general point of view, this is wrong as illustrated in Figure 5. Indeed, we have plotted in solid line the boundary of a set S which is the intersection of two identical disks' complements. This set is uniformly prox-regular but its constant of prox-regularity (equal to the radius of the disk plotted in dashed line) tends to zero when the disks' centres move away from each other. In this situation, the scalar product between normal vectors \mathbf{n}_1 and \mathbf{n}_2 (see Figure 6) tends to -1. Thus, the constant of prox-regularity of S is also dependent on the angle between vectors \mathbf{n}_1 and \mathbf{n}_2 . We now come to the main result of this subsection: the uniform prox-regularity of Q . This result rests on an inverse triangle inequality between vectors $\mathbf{G}_{ij}(\mathbf{q})$, which is based on angle estimates. Let us point out that we do not claim optimality of the constant η below.

Proposition 2.17 *Q is η -prox-regular with*

$$\eta \sim \frac{r\sqrt{2}}{2^{3N}} \frac{1}{12^{3N^2}}.$$

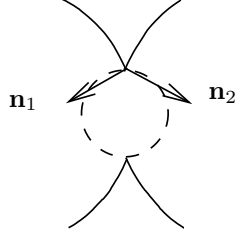


Figure 6: Evolution of the angle between vectors \mathbf{n}_1 and \mathbf{n}_2 .

Proof: We want to prove (cf. Proposition 2.5) that there exists $\eta > 0$ such that for all $\mathbf{q} \in Q$ and for all $\mathbf{v} \in N(Q, \mathbf{q})$,

$$\mathbf{v} \cdot (\tilde{\mathbf{q}} - \mathbf{q}) \leq \frac{|\mathbf{v}|}{2\eta} |\tilde{\mathbf{q}} - \mathbf{q}|^2, \quad \forall \tilde{\mathbf{q}} \in Q. \quad (7)$$

By Proposition 2.15, for all $\mathbf{q} \in Q_{ij}$ and all $\mathbf{w} \in N(Q_{ij}, \mathbf{q})$, we have

$$\mathbf{w} \cdot (\tilde{\mathbf{q}} - \mathbf{q}) \leq \frac{|\mathbf{w}|}{2\eta_0} |\tilde{\mathbf{q}} - \mathbf{q}|^2, \quad \forall \tilde{\mathbf{q}} \in Q_{ij}. \quad (8)$$

Inequality (7) is obvious when $\mathbf{v} = 0$. So we consider $\mathbf{q} \in \partial Q$ and $\mathbf{v} \in N(Q, \mathbf{q}) \setminus \{0\}$. By Proposition 2.16,

$$\mathbf{v} = - \sum_{(i,j) \in I_{\text{contact}}} \alpha_{ij} \mathbf{G}_{ij}(\mathbf{q}), \quad \alpha_{ij} \geq 0.$$

We recall that $Q \subset Q_{ij}$ so that by (8) we obtain

$$\left(- \sum \alpha_{ij} \mathbf{G}_{ij}(\mathbf{q}) \right) \cdot (\tilde{\mathbf{q}} - \mathbf{q}) \leq \sum \frac{\alpha_{ij} |\mathbf{G}_{ij}(\mathbf{q})|}{2\eta_0} |\tilde{\mathbf{q}} - \mathbf{q}|^2, \quad \forall \tilde{\mathbf{q}} \in Q.$$

The sum concerns only couples (i, j) belonging to I_{contact} but for convenience, this point is omitted in the notation. As $|\mathbf{G}_{ij}(\mathbf{q})| = \sqrt{2}$, we get

$$\mathbf{v} \cdot (\tilde{\mathbf{q}} - \mathbf{q}) \leq \frac{1}{\sqrt{2}\eta_0} \left(\sum \alpha_{ij} \right) |\tilde{\mathbf{q}} - \mathbf{q}|^2, \quad \forall \tilde{\mathbf{q}} \in Q.$$

To check Inequality (7), it suffices to find a constant $\eta > 0$, independent from α_{ij} and from \mathbf{q} , satisfying

$$\left(\sum \alpha_{ij} \right) \frac{1}{\sqrt{2}\eta_0} \leq \frac{1}{2\eta} \left| \sum \alpha_{ij} \mathbf{G}_{ij}(\mathbf{q}) \right|,$$

i.e. such that

$$\left| \sum \alpha_{ij} \mathbf{G}_{ij}(\mathbf{q}) \right| \geq \sqrt{2} \frac{\eta}{\eta_0} \left(\sum \alpha_{ij} \right).$$

Finally, if we are able to exhibit $\gamma > 0$ verifying

$$\left| \sum \alpha_{ij} \mathbf{G}_{ij}(\mathbf{q}) \right| \geq \frac{\sqrt{2}}{\gamma} \left(\sum \alpha_{ij} \right),$$

then Q will be η -prox-regular with

$$\eta = \frac{\eta_0}{\gamma} = \frac{r\sqrt{2}}{\gamma}.$$

The problem takes the form of an inverse triangle inequality:

$$\sum \alpha_{ij} |\mathbf{G}_{ij}(\mathbf{q})| = \sqrt{2} \sum \alpha_{ij} \leq \gamma \left| \sum \alpha_{ij} \mathbf{G}_{ij}(\mathbf{q}) \right|.$$

The required result will follow as soon as we prove the main proposition stated below. \square

Proposition 2.18 (Inverse triangle inequality)

There exists $\gamma > 1$ such that for all $\mathbf{q} \in Q$,

$$\sum_{(i,j) \in I_{\text{contact}}} \alpha_{ij} |\mathbf{G}_{ij}(\mathbf{q})| \leq \gamma \left| \sum_{(i,j) \in I_{\text{contact}}} \alpha_{ij} \mathbf{G}_{ij}(\mathbf{q}) \right|,$$

where

$$I_{\text{contact}} = \{(i, j), i < j, D_{ij}(\mathbf{q}) = 0\} \text{ and } \alpha_{ij} \text{ are nonnegative reals.}$$

Constant γ can be fixed as follows

$$\gamma = \left[\frac{1}{2} \left(1 - \left(1 + \left(\frac{1}{12^{2N}} \right) \right)^{-1/2} \right) \right]^{-\frac{3N}{2}}.$$

Remark 2.19 Note the sign of coefficients α_{ij} . From a general point of view, this inequality is obviously wrong if these coefficients are just assumed real. Indeed, for N large enough, the cardinal of the set I_{contact} could be strictly larger than $2N$, which induces a relation between vectors $\mathbf{G}_{ij}(\mathbf{q})$ (see Fig. 8 for such a degenerate situation).

The following elementary lemma asserts an inverse triangle inequality for two vectors.

Lemma 2.20 Let u_1 and u_2 be two vectors of \mathbb{R}^{2N} satisfying $u_1 \cdot u_2 = \cos \theta |u_1| |u_2|$, with $\cos \theta > -1$. Then for all

$$\nu \geq \nu_\theta := \sqrt{\frac{2}{1 + \cos \theta}}$$

we have $|u_1| + |u_2| \leq \nu |u_1 + u_2|$.

Proof of the inverse triangle inequality: We propose here a method based on angle estimates with vectors $\mathbf{G}_{ij}(\mathbf{q})$ as pointed out in Figure 6. We use a recursive proof on the number of involved vectors. We are going to check that there exists $\delta > 1$ such that for all subset $I \subset I_{\text{contact}}$ and for all $\alpha_{ij} > 0$,

$$\sum_{(i,j) \in I \subset I_{\text{contact}}} \alpha_{ij} |\mathbf{G}_{ij}(\mathbf{q})| \leq \delta^{|I|} \left| \sum_{(i,j) \in I \subset I_{\text{contact}}} \alpha_{ij} \mathbf{G}_{ij}(\mathbf{q}) \right|.$$

Initialization: Suppose that the cardinality of I equals to 1, in other words, $I = \{(i, j)\}$. So we clearly have for all $\alpha_{ij} > 0$ and all $\delta > 1$,

$$\alpha_{ij} |\mathbf{G}_{ij}(\mathbf{q})| = |\alpha_{ij} \mathbf{G}_{ij}(\mathbf{q})| \leq \delta |\alpha_{ij} \mathbf{G}_{ij}(\mathbf{q})|. \quad (9)$$

Recursion assumption:

If $|J| = p$, then we have for all $\alpha_{ij} > 0$

$$\sum_{(i,j) \in J \subset I_{\text{contact}}} \alpha_{ij} |\mathbf{G}_{ij}(\mathbf{q})| \leq \delta^p \left| \sum_{(i,j) \in J \subset I_{\text{contact}}} \alpha_{ij} \mathbf{G}_{ij}(\mathbf{q}) \right|. \quad (10)$$

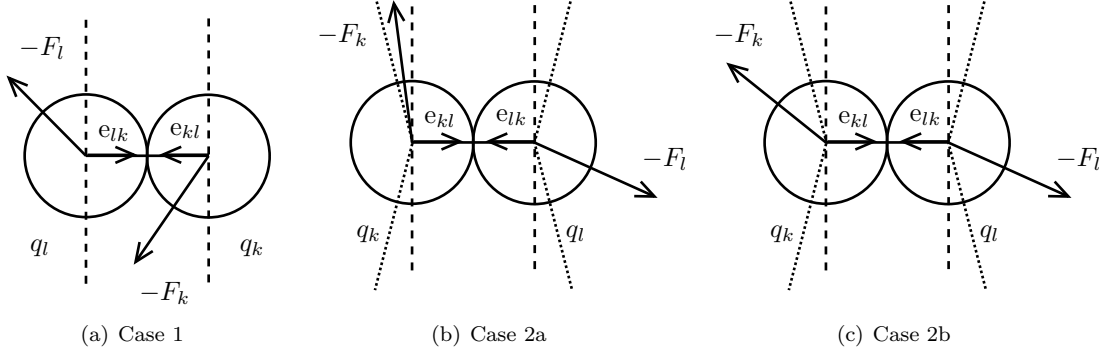
Take a subset $I \subset I_{\text{contact}}$ with $|I| = p + 1$. For any

$$\mathbf{w} = \sum_{(i,j) \in I} \alpha_{ij} \mathbf{G}_{ij}(\mathbf{q}),$$

with $\alpha_{ij} > 0$, we choose $(k, l) \in I$ and define $J = I \setminus \{(k, l)\}$,

$$\mathbf{w}_1 = \sum_{(i,j) \in J} \alpha_{ij} \mathbf{G}_{ij}(\mathbf{q}) \text{ and } \mathbf{w}_2 = \alpha_{kl} \mathbf{G}_{kl}(\mathbf{q}).$$

We need the following lemma which will be later proved.



Lemma 2.21 *If $\mathbf{w}_1 \neq 0$, the following inequality holds*

$$\frac{\mathbf{w}_1 \cdot \mathbf{w}_2}{|\mathbf{w}_1||\mathbf{w}_2|} \geq -\kappa, \text{ with } \kappa = \left(1 + \left(\frac{1}{12}\right)^{2N}\right)^{-1/2}.$$

Consequently, if $\mathbf{w}_1 \neq 0$, from Lemma 2.20, we deduce $|\mathbf{w}_1| + |\mathbf{w}_2| \leq \sqrt{\frac{2}{1-\kappa}}|\mathbf{w}_1 + \mathbf{w}_2|$ (this inequality obviously holds for $\mathbf{w}_1 = 0$). By denoting $\delta = \sqrt{\frac{2}{1-\kappa}} > 1$, we get

$$|\mathbf{w}_1| + |\mathbf{w}_2| \leq \delta|\mathbf{w}|. \quad (11)$$

Applying recursion assumption (10) and (11), we obtain

$$\sum_{(i,j) \in I_{\text{contact}}} \alpha_{ij} |\mathbf{G}_{ij}(\mathbf{q})| \leq \alpha_{kl} |\mathbf{G}_{kl}(\mathbf{q})| + \delta^p |\mathbf{w}_1| \leq \delta^p (|\mathbf{w}_2| + |\mathbf{w}_1|) \leq \delta^{p+1} |\mathbf{w}|,$$

which ends the proof of (9) by recursion. As $|I_{\text{contact}}| \leq 3N$, the inverse triangle inequality is checked with $\gamma = \delta^{3N}$. \square

Proof of Lemma 2.21: It suffices to deal with $\mathbf{w}_2 = \mathbf{G}_{kl}(\mathbf{q})$. By setting

$$\beta_{ij} = \begin{cases} \alpha_{ij} & \text{if } i < j \\ \alpha_{ji} & \text{else,} \end{cases}$$

we have

$$\mathbf{w}_1 = (F_1, F_2, \dots, F_N) \text{ where } F_p = \sum \beta_{ip} e_{ip}.$$

Thus, $F_k \in \mathbb{R}^2$ can be interpreted as a pressure force exerted on the k^{th} person by its neighbours (different from the individual l). Similarly, $-F_k$ can be seen as a reaction force. We are looking for a lower bound of

$$\Delta_{kl} := \frac{\mathbf{w}_1 \cdot \mathbf{w}_2}{|\mathbf{w}_1||\mathbf{w}_2|} = \frac{-F_k \cdot e_{kl} - F_l \cdot e_{lk}}{\sqrt{2} \sqrt{\sum_{i=1}^N |F_i|^2}}.$$

Case 1: $-F_k \cdot e_{kl} \geq 0$ or $-F_l \cdot e_{lk} \geq 0$

Suppose that, for example (cf figure 7(a)) $-F_k \cdot e_{kl} \geq 0$. Using $|F_l \cdot e_{lk}| \leq |F_l|$, we get

$$\Delta_{kl} \geq \frac{-F_l \cdot e_{lk}}{\sqrt{2} \sqrt{\sum |F_i|^2}} \geq \frac{-1}{\sqrt{2}}.$$

In this case, $\kappa = 2^{-1/2}$.

Case 2: $-F_k \cdot e_{kl} < 0$ and $-F_l \cdot e_{lk} < 0$

Case 2a: $-F_k \cdot e_{kl} \geq -\frac{1}{4}|F_k|$ or $-F_l \cdot e_{lk} \geq -\frac{1}{4}|F_l|$

Suppose that, for example (cf Figure 7(b)), $-F_k \cdot e_{kl} \geq -\frac{1}{4}|F_k|$. It can be shown that

$$-\frac{1}{4} \leq \frac{-F_k \cdot e_{kl}}{\sqrt{\sum |F_i|^2}} \text{ and } \frac{-F_l \cdot e_{lk}}{\sqrt{\sum |F_i|^2}} \geq -1,$$

which yields

$$\Delta_{kl} \geq \frac{1}{\sqrt{2}} \left(-\frac{1}{4} - 1 \right) = -\frac{5}{4\sqrt{2}} > -1.$$

In this case $\kappa = 5/(4\sqrt{2})$.

Case 2b: $-F_k \cdot e_{kl} < -\frac{1}{4}|F_k|$ and $-F_l \cdot e_{lk} < -\frac{1}{4}|F_l|$ (cf Figure 7(c)).

We need the following lemma.

Lemma 2.22 *There exists \tilde{k} and \tilde{l} different from k and l verifying $\tilde{k} \neq \tilde{l}$ and*

$$\begin{aligned} |F_{\tilde{k}}| &\geq \epsilon |F_k|, \\ |F_{\tilde{l}}| &\geq \epsilon |F_l|, \end{aligned}$$

with $\epsilon = 1/12^{2N}$.

We deduce that

$$\sum |F_i|^2 \geq |F_k|^2 + |F_l|^2 + |F_{\tilde{k}}|^2 + |F_{\tilde{l}}|^2 \geq (1 + \epsilon^2) [|F_k|^2 + |F_l|^2].$$

Therefore

$$|\Delta_{kl}| \leq \frac{1}{\sqrt{1 + \epsilon^2}} \left(\frac{|F_k| + |F_l|}{\sqrt{2}\sqrt{|F_k|^2 + |F_l|^2}} \right) \leq \frac{1}{\sqrt{1 + \epsilon^2}}.$$

In this case, $\kappa = \frac{1}{\sqrt{1 + \epsilon^2}}$, which concludes the proof of Lemma 2.21. □

Proof of Lemma 2.22: We firstly consider

$$-F_k = \sum_{i=1}^{V_k} \beta_{kj_0,i} e_{kj_0,i},$$

where V_k is the number of neighbours of individual k (individual l excepted) ($V_k \leq 5$). As a consequence,

$$-F_k \cdot e_{kl} = \sum_{i=1}^{V_k} \beta_{kj_0,i} e_{kj_0,i} \cdot e_{kl}.$$

There exists $k_1 \in \{j_{0,1}, j_{0,2}, \dots, j_{0,V_k}\}$ ($k_1 \neq k, l$) such that for all $i \in \{1, \dots, V_k\}$ $\beta_{kk_1} e_{kk_1} \cdot e_{kl} \leq \beta_{kj_0,i} e_{kj_0,i} \cdot e_{kl}$. It is obvious that

$$\beta_{kk_1} e_{kk_1} \cdot e_{kl} < -\frac{1}{6} F_k \cdot e_{kl} \leq -\frac{1}{24} |F_k|.$$

In fact, individual k_1 is the neighbour who exerts the largest pressure force on person k . As illustrated in Figure 7, individual k is between persons l and k_1 .

If $|F_{k_1}| \geq \frac{1}{48} |F_k|$, then we set $\tilde{k} = k_1$. Else $|F_{k_1}| < \frac{1}{48} |F_k|$, and we produce the same reasoning with

$$-F_{k_1} = \beta_{k_1 k} e_{k_1 k} + \sum_{i=1}^{V_{k_1}} \beta_{k_1 j_1,i} e_{k_1 j_1,i},$$

where $V_{k_1} \leq 5$. Thus,

$$-F_{k_1} \cdot e_{kl} = \beta_{k_1 k} e_{k_1 k} \cdot e_{kl} + \sum_{i=1}^{V_{k_1}} \beta_{k_1 j_1,i} e_{k_1 j_1,i} \cdot e_{kl}.$$

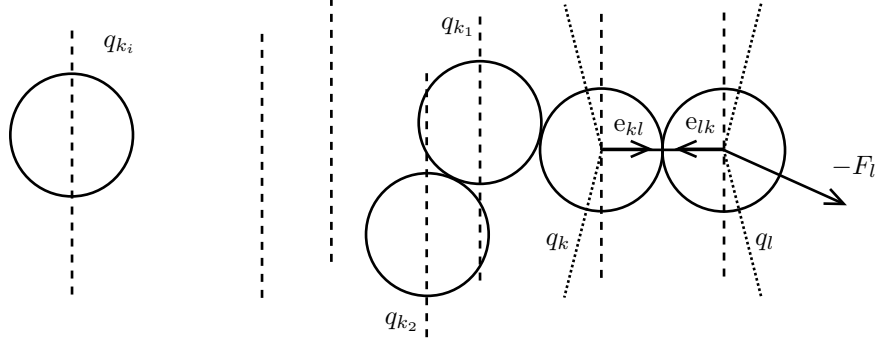


Figure 7: Construction of sequence (k_i)

Since $-\beta_{k_1 k} e_{k_1 k} \cdot e_{kl} < -\frac{1}{24}|F_k|$ and $-F_{k_1} \cdot e_{kl} \leq |F_{k_1}| < \frac{1}{48}|F_k|$, we obtain

$$\sum_{i=1}^{V_{k_1}} \beta_{k_1 j_{1,i}} e_{k_1 j_{1,i}} \cdot e_{kl} = -F_{k_1} \cdot e_{kl} - \beta_{k_1 k} e_{k_1 k} \cdot e_{kl} < -\frac{1}{48}|F_k|.$$

As previously, there exists $k_2 \in \{j_{1,1}, j_{1,2}, \dots, j_{1,V_{k_1}}\}$ ($k_2 \notin \{k, k_1\}$), such that

$$\beta_{k_1 k_2} e_{k_1 k_2} \cdot e_{kl} < -\frac{1}{4 \times 12^2}|F_k|$$

(Similarly, see Figure 7, individual k_1 is between persons k_2 and k).

If $|F_{k_2}| \geq \frac{1}{4} \left(\frac{1}{12}\right)^2 |F_k|$, we set $\tilde{k} = k_2$. Else, we continue by defining a sequence (k_i) (cf Figure 7) such that

$$\begin{cases} k_0 = k \\ |F_{k_{i+1}}| < \frac{1}{4} \left(\frac{1}{12}\right)^{i+1} |F_k| \\ \beta_{k_i k_{i+1}} e_{k_i k_{i+1}} \cdot e_{kl} < -\frac{1}{4} \left(\frac{1}{12}\right)^i \frac{1}{6} |F_k|. \end{cases}$$

It can be shown that $k_{i+1} \notin \{k_0, k_1, \dots, k_i\}$. This construction ends at most in $N - 2$ steps:

$$\exists m < N - 1 \text{ satisfying } |F_{k_m}| \geq \frac{1}{4} \left(\frac{1}{12}\right)^m |F_k|.$$

Finally we set

$$\tilde{k} = k_m.$$

Analogously, we deal with F_l , by constructing a sequence (l_i) verifying similar properties. We can check that $\tilde{k} \neq \tilde{l}$ in proving that

$$\{k_0, k_1, \dots, k_m\} \cap \{l_0, l_1, \dots, l_p\} = \emptyset.$$

The proof of Lemma 2.22 is achieved by taking $\epsilon = 1/12^N$. \square

3 Numerical scheme

3.1 Time-discretization scheme

We present in this section a numerical scheme to approximate the solution to (5). The numerical scheme we propose is based on a first order expansion of the constraints expressed in terms of velocities. The time interval

is denoted by $[0, T]$. Let $N \in \mathbb{N}^*$, $h = T/N$ be the time step and $t^n = nh$ be the computational times. We denote by \mathbf{q}^n the approximation of $\mathbf{q}(t^n)$. The next configuration is obtained as

$$\mathbf{q}^{n+1} = \mathbf{q}^n + h \mathbf{u}^n,$$

where

$$\mathbf{u}^n = \text{P}_{\mathcal{C}_{\mathbf{q}}^h}(\mathbf{U}(\mathbf{q}^n)) \text{ with}$$

$$\mathcal{C}_{\mathbf{q}}^h = \{\mathbf{v} \in \mathbb{R}^{2N}, D_{ij}(\mathbf{q}) + h \mathbf{G}_{ij}(\mathbf{q}) \cdot \mathbf{v} \geq 0 \quad \forall i < j\}.$$

The scheme can be also interpreted in the following way. Let us introduce the set

$$\tilde{Q}(\mathbf{q}) = \{\tilde{\mathbf{q}} \in \mathbb{R}^{2N}, D_{ij}(\mathbf{q}) + \mathbf{G}_{ij}(\mathbf{q}) \cdot (\tilde{\mathbf{q}} - \mathbf{q}) \geq 0 \quad \forall i < j\},$$

which can be seen as an inner convex approximation of Q with respect to \mathbf{q} . Note that $\tilde{Q}(\mathbf{q})$ is defined in such a way that Q is the union of all sets $\tilde{Q}(\mathbf{q})$, $\mathbf{q} \in Q$. The scheme can be expressed in terms of position:

$$\mathbf{q}^{n+1} = \text{P}_{\tilde{Q}(\mathbf{q}^n)}(\mathbf{q}^n + h\mathbf{U}(\mathbf{q}^n)).$$

In this form it appears as a prediction-correction algorithm: predicted position vector $\mathbf{q}^n + h\mathbf{U}(\mathbf{q}^n)$, that may not be admissible, is projected onto the approximate set of feasible configurations.

Remark 3.1 *It is straightforward to check that*

$$\frac{\mathbf{q}^{n+1} - \mathbf{q}^n}{h} + \text{N}(\tilde{Q}(\mathbf{q}^n), \mathbf{q}^{n+1}) \ni \mathbf{U}(\mathbf{q}^n), \quad (12)$$

so that the scheme can also be seen as a semi-implicit discretization of (5), where $\text{N}(\tilde{Q}(\mathbf{q}^n), \mathbf{q}^{n+1})$ approximates $\text{N}(Q, \mathbf{q}^n)$.

Convergence of this scheme shall be proven in a forthcoming paper.

3.2 Numerical solutions

In the model, the discrete actual velocity \mathbf{u}^n is the projection of the spontaneous velocity onto the approximated set of feasible velocities. We propose here to solve this projection by a Uzawa algorithm (note that any algorithm could be used to perform this task). For convenience, explicit dependence of vectors and matrices upon the current configuration is omitted (e.g. \mathbf{U} stands for $\mathbf{U}(\mathbf{q}^n)$, D_{ij} for $D_{ij}(\mathbf{q}^n)$, etc...). The actual velocity \mathbf{u} solves the following minimization problem under constraints

$$\mathbf{u} = \underset{\mathbf{v} \in \mathcal{C}_{\mathbf{q}}^h}{\text{argmin}} |\mathbf{v} - \mathbf{U}|^2.$$

Uzawa algorithm is based on a reformulation of this minimization problem in a saddle-point form. We introduce the associated Lagrangian

$$L(\mathbf{v}, \boldsymbol{\mu}) = \frac{1}{2} |\mathbf{v} - \mathbf{U}|^2 - \sum_{1 \leq i < j \leq N} \mu_{ij} (D_{ij} + h \mathbf{G}_{ij} \cdot \mathbf{v}).$$

and the following linear mapping

$$\begin{aligned} B : \mathbb{R}^{2N} &\rightarrow \mathbb{R}^{\frac{N(N-1)}{2}} \\ \mathbf{v} &\mapsto -h (\mathbf{G}_{ij} \cdot \mathbf{v})_{i < j} \end{aligned}$$

With these notations, the set $\mathcal{C}_{\mathbf{q}}^h$ can be written:

$$\begin{aligned} \mathcal{C}_{\mathbf{q}}^h &= \left\{ \mathbf{v} \in \mathbb{R}^{2N}, \forall \boldsymbol{\mu} \in (\mathbb{R}^+)^{\frac{N(N-1)}{2}}, - \sum_{1 \leq i < j \leq N} \mu_{ij} (D_{ij} + h \mathbf{G}_{ij} \cdot \mathbf{v}) \leq 0 \right\} \\ &= \left\{ \mathbf{v} \in \mathbb{R}^{2N}, \forall \boldsymbol{\mu} \in (\mathbb{R}^+)^{\frac{N(N-1)}{2}}, \boldsymbol{\mu} \cdot (B\mathbf{v} - D) \leq 0 \right\}. \end{aligned}$$

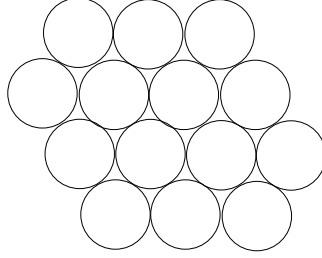


Figure 8: A case of non-uniqueness for Kuhn-Tucker multipliers.

where $D = D(\mathbf{q}) \in \mathbb{R}^{N(N-1)/2}$ is the vector of distances. The existence of a saddle-point

$$(\mathbf{u}, \boldsymbol{\lambda}) \in \mathbb{R}^{2N} \times (\mathbb{R}^+)^{\frac{N(N-1)}{2}}$$

for this problem is well-known (see e.g. [8]) and it is characterized by the next system:

$$\begin{cases} \mathbf{u} + {}^t B \boldsymbol{\lambda} = \mathbf{U} \\ \boldsymbol{\mu} \cdot (B \mathbf{u} - D) \leq 0, \quad \forall \boldsymbol{\mu} \geq 0 \\ \boldsymbol{\lambda} \cdot (B \mathbf{u} - D) = 0. \end{cases}$$

Uzawa algorithm produces two sequences $(\mathbf{v}^k) \in (\mathbb{R}^{2N})^{\mathbb{N}}$ and $(\boldsymbol{\mu}^k) \in ((\mathbb{R}^+)^{\frac{N(N-1)}{2}})^{\mathbb{N}}$ according to

$$\begin{aligned} \boldsymbol{\mu}^0 &= 0 \\ \mathbf{v}^{k+1} &= \mathbf{U} - {}^t B \boldsymbol{\mu}^k \\ \boldsymbol{\mu}^{k+1} &= \Pi_+ (\boldsymbol{\mu}^k + \rho [B \mathbf{v}^{k+1} - D]), \end{aligned}$$

where Π_+ is the euclidean projection onto the cone of vectors with nonnegative components (a simple cut-off in practice), and $\rho > 0$ is a fixed parameter. The algorithm can be shown to converge as soon as $0 < \rho < 2/\|B\|^2$ (see [8]). More precisely, the sequence (\mathbf{v}^k) converges to \mathbf{u} and it can be shown that the sequence $(\boldsymbol{\mu}^k)$ tends to some $\bar{\boldsymbol{\lambda}} \in (\mathbb{R}^+)^{\frac{N(N-1)}{2}}$ such that $(\mathbf{u}, \bar{\boldsymbol{\lambda}})$ is a saddle-point of L . Notice that in general, the Kuhn-Tucker multiplier $\boldsymbol{\lambda}$ is not unique as illustrated in Figure 8. In this case, the configuration of 14 people shows 29 contacts, consequently matrix ${}^t B$ is not injective.

Remark 3.2 (*Link between local prox-regularity and speed of convergence for Uzawa algorithm*) We denote by G the matrix whose columns are vectors \mathbf{G}_{ij} , where $(i, j) \in I_{\text{contact}}$ (defined by (6)), and we introduce $A = {}^t G G$. The size of this square matrix is equal to n_{contact} which is the cardinal of I_{contact} . By inverse triangle inequality (see Proposition 2.18), there exists a constant γ such that for all $\boldsymbol{\lambda} \in (\mathbb{R}^+)^{n_{\text{contact}}}$ satisfying $|\boldsymbol{\lambda}|_1 = 1$, we have

$$\left| \sum \lambda_{ij} \mathbf{G}_{ij} \right|^2 = {}^t \boldsymbol{\lambda} {}^t G G \boldsymbol{\lambda} = {}^t \boldsymbol{\lambda} A \boldsymbol{\lambda} \geq \frac{2}{\gamma^2}.$$

We define, for $\mathbf{q} \in Q$, a local parameter $\gamma_{\mathbf{q}}$ satisfying

$$\min_{\substack{|\boldsymbol{\lambda}|_1=1 \\ \boldsymbol{\lambda} \geq 0}} {}^t \boldsymbol{\lambda} A \boldsymbol{\lambda} = \frac{2}{\gamma_{\mathbf{q}}^2},$$

and $\eta_{\mathbf{q}} = r\sqrt{2}/\gamma_{\mathbf{q}}$. Let us show that parameter $\eta_{\mathbf{q}}$ (setting a lower bound of the local prox-regularity of Q at point \mathbf{q}) and the condition number of matrix A are closely related when A is non-singular. By denoting η_{\min} the smallest eigenvalue of A , it follows that

$$\eta_{\min} = \min_{|\boldsymbol{\lambda}|_2=1} {}^t \boldsymbol{\lambda} A \boldsymbol{\lambda} = \min_{|\boldsymbol{\lambda}|_2 \geq 1} {}^t \boldsymbol{\lambda} A \boldsymbol{\lambda} \leq \min_{\substack{|\boldsymbol{\lambda}|_2 \geq 1 \\ \boldsymbol{\lambda} \geq 0}} {}^t \boldsymbol{\lambda} A \boldsymbol{\lambda}.$$

Since for all $\boldsymbol{\lambda}$, $|\boldsymbol{\lambda}|_1 \leq \sqrt{n_{\text{contact}} |\boldsymbol{\lambda}|_2}$, we have

$$\min_{\substack{|\boldsymbol{\lambda}|_2 \geq 1 \\ \boldsymbol{\lambda} \geq 0}} {}^t \boldsymbol{\lambda} A \boldsymbol{\lambda} \leq \min_{\substack{|\boldsymbol{\lambda}|_1 \geq \sqrt{n_{\text{contact}}} \\ \boldsymbol{\lambda} \geq 0}} {}^t \boldsymbol{\lambda} A \boldsymbol{\lambda} = n_{\text{contact}} \min_{\substack{|\boldsymbol{\lambda}|_1 \geq 1 \\ \boldsymbol{\lambda} \geq 0}} {}^t \boldsymbol{\lambda} A \boldsymbol{\lambda}.$$

Finally,

$$\eta_{min} \leq n_{contact} \min_{\substack{|\lambda|_1 \geq 1 \\ \lambda \geq 0}} {}^t \lambda A \lambda = n_{contact} \min_{\substack{|\lambda|_1 = 1 \\ \lambda \geq 0}} {}^t \lambda A \lambda = \frac{2n_{contact}}{\gamma_{\mathbf{q}}^2}.$$

Thus

$$\eta_{min} \leq \frac{6N}{\gamma_{\mathbf{q}}^2}.$$

Furthermore, the condition number of matrix A equals to

$$\text{cond}_2(A) = \|A\|_2 \|A^{-1}\|_2 = \frac{\eta_{max}}{\eta_{min}}.$$

Since $|\mathbf{G}_{ij}(\mathbf{q})| = \sqrt{2}$, we obtain $\|A\|_2 = \eta_{max} \geq 2$, hence

$$\text{cond}_2(A) \geq \frac{2}{\eta_{min}} \geq \frac{2\gamma_{\mathbf{q}}^2}{6N} \geq \frac{4r^2}{6\eta_{\mathbf{q}}^2 N},$$

which quantifies how the condition number of A varies with $\eta_{\mathbf{q}}$. Since the matrix appearing in Uzawa algorithm is $A = {}^t G G$, we expect that this algorithm converges less quickly for configurations with low local prox-regularity. In numerical simulations, we noticed indeed that solving the saddle-point problem requires more iterations in case of a jam.

4 Numerical results

In order to illustrate the contact model, we propose here an example of spontaneous velocity. The choice of the spontaneous velocity is important because this velocity reflects pedestrian behaviour. A lot of choices are obviously possible. The spontaneous velocity of an individual has to take into account obstacles in the room and specify how he wants to get around them. So this velocity depends on the room's geometry but it can be made dependent on other people positions too. Indeed, it is possible here to integrate individual strategies (deceleration or jam's avoiding). We refer the reader to [32, 33, 42] for other examples of spontaneous velocity. Here we restrict ourselves to simple behavioural model: people tend to optimize their own path, regardless of others.

An example of spontaneous velocity

We consider here the simplest choice for the spontaneous velocity. All the individuals have the same behaviour: they want to reach the exit by following the shortest path avoiding obstacles. Then, the spontaneous velocity's expression can be specified:

$$\mathbf{U}(\mathbf{q}) = (\mathbf{U}_0(\mathbf{q}_1), \dots, \mathbf{U}_0(\mathbf{q}_N)) \text{ with } \mathbf{U}_0(\mathbf{x}) = -s \nabla \mathcal{D}(\mathbf{x}),$$

where $\mathcal{D}(\mathbf{x})$ represents the geodesic distance between the position \mathbf{x} and the nearest exit and $s > 0$ denotes the speed. In order to compute \mathcal{D} , we have used the Fast Marching Method introduced by R. Kimmel and J. Sethian in [27]. In this method, the value of \mathcal{D} is computed at each point of a grid. The value at the exit's nodes is set to zero. Then, the values of the distance at the other points is computed step by step so that a discrete version of $|\nabla \mathcal{D}| = 1$ is satisfied. Moreover, the distance at the nodes situated in the obstacles is fixed to a large value, which prevents the shortest path from going across them. In Figure 9, we have considered a room with 5 obstacles and the exit is situated to the left. We note that by following the built velocity field, people are going to avoid obstacles.

Our aim is to simulate evacuation of any building consisting of several floors. We have chosen an object oriented programming method and we have implemented this Fast Marching Method in a C++ code. Let us detail this code. On each floor, the spontaneous velocity is directed by the shortest path avoiding obstacles to the nearest exit or stairwell. In the stairs, people just want to go down. We have integrated this spontaneous velocity in the C++ code SCoPI: Simulations of Collections of Interacting Particles developed by A. Lefebvre (see [29, 30]). This code allows us to compute the actual velocity as the projection of the spontaneous velocity as described in Section 3.

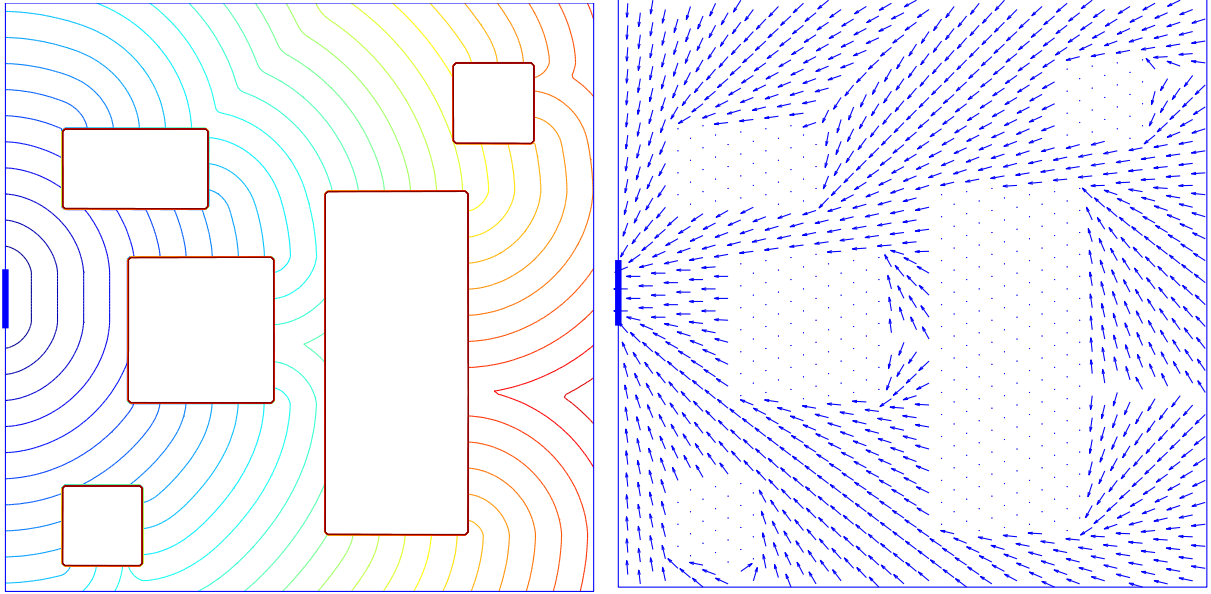


Figure 9: Contour levels of the geodesic distance \mathcal{D} and velocity field \mathbf{U}_0 .

Remark 4.1 Notice that the velocity field produced by this strategy is not continuous as soon as the room is not convex, which rules out Theorem 2.10. This lack of regularity is not important in practical applications : the places at which it occurs (in particular upstream obstacles) are emptied after a few moments. The main consequence is the discontinuity of the future configurations with respect to initial data, which is not surprising from a modelling standpoint.

We propose to illustrate the behaviour of the algorithm in two situations. The first one corresponds to a many-individual evacuation from a square room through a single exit, the second one illustrate the capability of the approach to handle complicated geometries. For these two experiments, it will be noticed that the contacts between the individuals and the obstacles have to be handled (as the contacts between people). Even if an individual want to avoid an obstacle, he can be pushed on it by people behind them.

Simple evacuation

We consider the situation of 1000 people which are randomly distributed over a square room. The spontaneous velocity field corresponds straight pathlines towards the exit at constant speed. As the field has a negative divergence, it tends to increase the local density, so that congestion is rapidly reached in the neighbourhood of the exit, and the congestion front propagated upstream as long as it is feeded by incoming people. In Figure 11, we represented the current configuration and the corresponding network of interaction pressures: for any couple of disks in contact, we represent the segment between centers, having its color (from white to black) depend upon the (positive) Kuhn-Tucker multiplier which handles the corresponding constraint. We recover the apparition of arches upstream the exit. The Kuhn-Tucker multipliers λ_{ij} quantify the way \mathbf{U} , the spontaneous velocity field, does not fit the constraints, and as such they can be interpreted in terms of pressures undergone by individuals. Although it would be presumptuous at this stage to assimilate λ_{ij} to an actual measure of the discomfort experienced by persons i and j , it is obvious that high values for those Kuhn-Tucker multipliers can be expected on zones where people are likely to be crushed.

Complex geometry

In the second example we consider the evacuation of a floor through exit stairs. A zoom on the geometry near the exit (together with the isovalues of the geodesic distance function, on which the spontaneous velocity is built) is represented on Figure 10. Figure 12 corresponds to snapshots at times 0s, 5s, 11s, 16s, 41s and 75s. Disks are colored according to their initial geodesic distance to the exit. Note that initial ordering is not preserved during the evacuation. Notice also how a jam forms between snapshots 2 and 3 in the room located on the left hand side. This jam decreases significantly the rate at which people exit the room, but it disappears

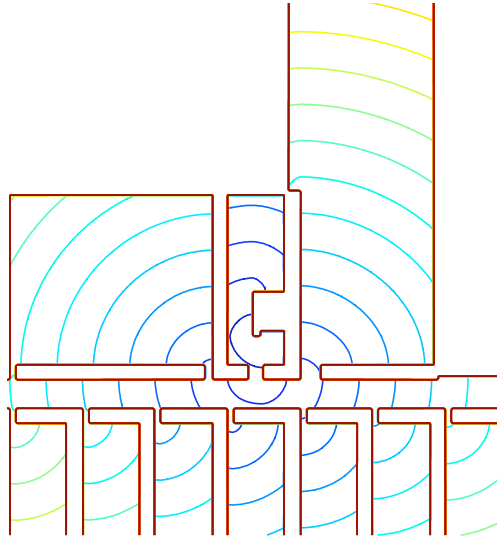


Figure 10: Geometry and isovalues for the geodesic distance.

eventually. The final evacuation time is 109s, to be compared to 48s which corresponds to the evacuation time without congestion.

References

- [1] F. Bernicot and J. Venel. Existence of sweeping process in banach spaces under directional prox-regularity. *submitted*, 2008.
- [2] V. Blue and J.L. Adler. Cellular automata microsimulation for modeling bi-directional pedestrian walkways. *Transportation Research B*, 35:293–312, 2001.
- [3] A. Borgers and H. Timmermans. City centre entry points, store location patterns and pedestrian route choice behaviour: A microlevel simulation model. *Socio-Economic Planning Sciences*, 20:25–31, 1986.
- [4] A. Borgers and H. Timmermans. A model of pedestrian route choice and demand for retail facilities within inner-cityshopping areas. *Geographical Analysis*, 18:115–128, 1986.
- [5] M. Bounkhel and L. Thibault. On various notions of regularity of sets in nonsmooth analysis. *Nonlinear Convex Anal.*, 48:223–246, 2002.
- [6] H. Brezis. *Opérateurs Maximaux Monotones et Semi-groupes de contractions dans les espaces de Hilbert*. AM, North Holland, 1973.
- [7] C. Burstedde, K. Klauck, A. Schadschneider, and J. Zittartz. Simulation of pedestrian dynamics using a two-dimensional cellular automaton. *Physica A*, 295:507–525, 2001.
- [8] P.G. Ciarlet. *Introduction à l'analyse numérique matricielle et à l'optimisation*. Masson, Paris, 1990.
- [9] F.H. Clarke, Y.S. Ledyev, R.J. Stern, and P.R. Wolenski. *Nonsmooth Analysis and Control Theory*. Springer-Verlag, New York, Inc., 1998.
- [10] F.H. Clarke, R.J. Stern, and P.R. Wolenski. Proximal smoothness and the lower- c^2 property. *J. Convex Anal.*, 2:117–144, 1995.

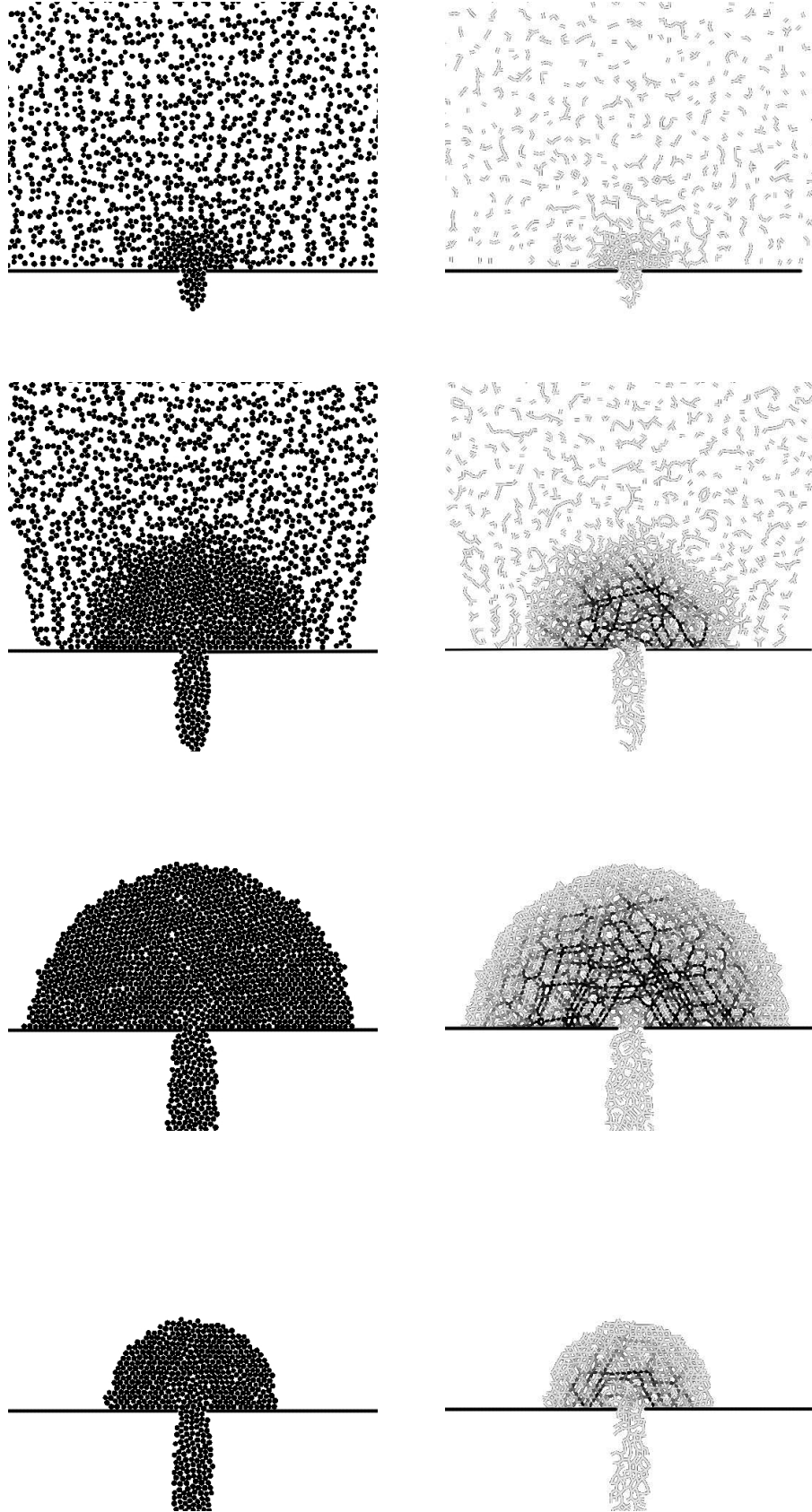


Figure 11: Arches.

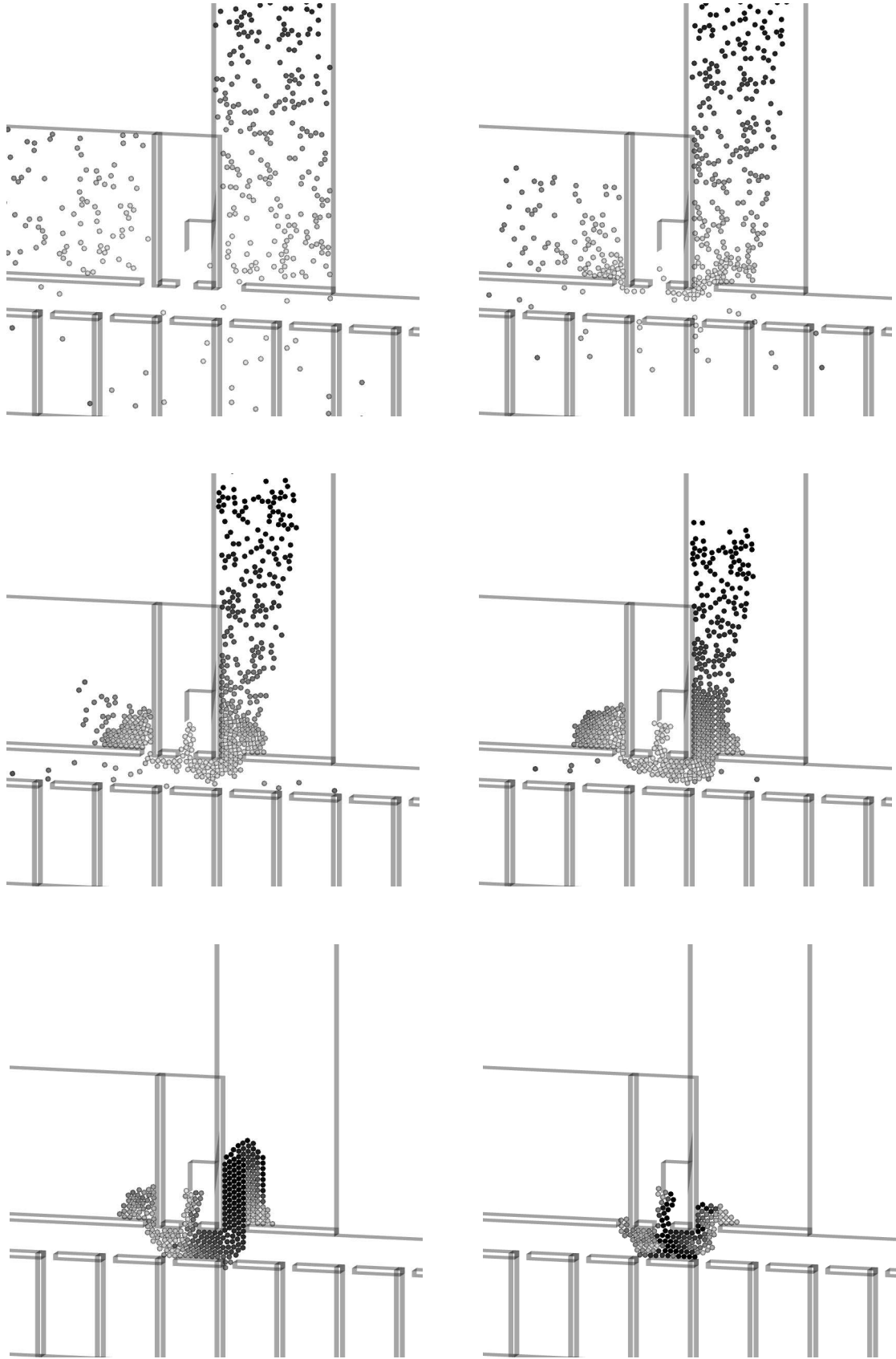


Figure 12: Zoom.

- [11] W. Daamen. *Modelling passenger flows in public transport facilities*. PhD thesis, Technische Universiteit Delft, 2004.
- [12] J.A. Delgado. Blaschke’s theorem for convex hypersurfaces. *J.Differential Geometry*, 14:489–496, 1979.
- [13] J.F. Edmond and L. Thibault. Relaxation of an optimal control problem involving a perturbed sweeping process. *Math. Program, Ser. B*, 104(2-3):347–373, 2005.
- [14] J.F. Edmond and L. Thibault. BVsolutions of nonconvex sweeping process differential inclusion with perturbation. *J. Differential Equations*, 226(1):135–179, 2006.
- [15] J.J. Fruin. Design for pedestrians: A level-of-service concept. *Highway Research Record*, 355:1–15, 1971.
- [16] S. Gwynne, E.R. Galea, P.J. Lawrence, and L. Filippidis. Modelling occupant interaction with fire conditions using the buildingexodus evacuation model. *Fire safety journal*, 36(4):327–357, 2001.
- [17] D. Helbing. A fluid-dynamic model for the movement of pedestrians. *Complex Systems*, 6:391–415, 1992.
- [18] D. Helbing, I.J. Farkas, and T. Vicsek. Simulating dynamical features of escape panic. *Nature*, 407:487, 2000.
- [19] D. Helbing and P. Molnár. Social force model for pedestrians dynamics. *Physical Review E*, 51:4282–4286, 1995.
- [20] L.F. Henderson. The stastitics of crowd fluids. *Nature*, 229:381–383, 1971.
- [21] H.Klüpfel and T. Meyer-König. Characteristics of the pedgo software for crowd movement and egress simulation. In E. Galea, editor, *Pedestrian and Evacuation Dynamics 2003*, pages 331–340, University of Greenwich, 2003. CMS Press, London.
- [22] S.P. Hoogendoorn and P.H.L. Bovy. Gas-kinetic modeling and simulation of pedestrian flows. *Transportation Research Record*, 1710:28–36, 2000.
- [23] S.P. Hoogendoorn and P.H.L. Bovy. Dynamic user-optimal assignment in continuous time and space. *Transportation Research B*, 38:571–592, 2004.
- [24] S.P. Hoogendoorn and P.H.L. Bovy. Pedestrian route-choice and activity scheduling theory and models. *Transportation Research B*, 38:169–190, 2004.
- [25] R. Hughes. The flow of large crowds of pedestrians. *Mathematics and Computers in Simulation*, 53:367–370, 2000.
- [26] R. Hughes. A continuum theory for the flow of pedestrians. *Transportation Research B*, 36(6):507–535, 2002.
- [27] R. Kimmel and J. Sethian. Fast marching methods for computing distance maps and shortest paths. Technical Report 669, CPAM,Univ. of California, Berkeley, 1996.
- [28] A. Kirchner and A. Schadschneider. Simulation of evacuation processes using a bionics-inspired cellular automaton model for pedestrians dynamics. *Physica A*, 312:260–276, 2002.
- [29] A. Lefebvre. *Modélisation numérique d’écoulements fluide/particules, Prise en compte des forces de lubrification*. PhD thesis, Université Paris-Sud XI, Faculté des sciences d’Orsay, 2007.
- [30] A. Lefebvre. Numerical simulations of gluey particles. To appear in M2AN, 2008.
- [31] G.G. Løvås. Modelling and simulation of pedestrian traffic flow. *Transportation Research B*, 28:429–443, 1994.
- [32] B. Maury and J. Venel. Un modèle de mouvement de foule. In *ESAIM: Proc.*, volume 18, pages 143–152, 2007.
- [33] B. Maury and J. Venel. Handling of contacts on crowd motion simulations. In *Traffic and Granular Flow ’07*. Springer, 2009. To appear.

- [34] J.J. Moreau. Décomposition orthogonale d'un espace hilbertien selon deux cônes mutuellement polaires. *C. R. Acad. Sci, Ser. I*, 255:238–240, 1962.
- [35] J.J. Moreau. Evolution problem associated with a moving convex set in a *Hilbert* space. *J. Differential Equations*, 26(3):347–374, 1977.
- [36] K. Nagel. From particle hopping models to traffic flow theory. *Transportation Research Record*, 1644:1–9, 1998.
- [37] P.D. Navin and R.J. Wheeler. Pedestrian flow characteristics. *Traffic Engineering*, 39:31–36, 1969.
- [38] A. Schadschneider. Cellular automaton approach to pedestrian dynamics-theory. In M. Schreckenberg and S. D. Sharma, editors, *Pedestrian and Evacuation Dynamics*, pages 75–85. Springer Berlin, 2001.
- [39] A. Schadschneider, A. Kirchner, and K. Nishinari. From ant trails to pedestrian dynamics. *Applied Bionics and Biomechanics*, 1:11–19, 2003.
- [40] G.K. Still. New computer system can predict human behavior response to building fires. *Fire*, 84:40–41, 1993.
- [41] J. Venel. *Modélisation mathématique et numérique des mouvements de foule*. PhD thesis, Université Paris-Sud XI, available at <http://tel.archives-ouvertes.fr/tel-00346035/fr>, 2008.
- [42] J. Venel. Integrating strategies in numerical modelling of crowd motion. In *Pedestrian and Evacuation Dynamics '08*. Springer, 2009. To appear.
- [43] U. Weidmann. Transporttechnik der fussgaenger. Technical Report 90, Schriftenreihe des Instituts für Verkehrsplanung, Transporttechnik, Strassen-und Eisenbahnbau, ETH Zürich, Switzerland, 1993.
- [44] S.J. Yuhaski and J.M. Macgregor Smith. Modelling circulation systems in buildings using state dependent queueing models. *Queueing Systems*, 4:319–338, 1989.